Solar Energy Materials & Solar Cells 277 (2024) 113048

Contents lists available at ScienceDirect

Solar Energy Materials and Solar Cells

journal homepage: www.elsevier.com/locate/solmat

Towards fiber-reinforced front-sheets for lightweight PV modules in VIPV

Marc Andre Schüler *, Mark-David Goth, Jochen Markert, Luis Eduardo Alanis, Christoph Kutter, Felix Basler, Martin Heinrich, Dirk Holger Neuhaus

Fraunhofer Institute for Solar Energy Systems (ISE), Heidenhofstrasse 2, 79110, Freiburg, Germany

ARTICLE INFO

Keywords:
Lightweight photovoltaics
Fiber reinforced plastics
Integrated PV (XIPV)

ABSTRACT

Novel approaches in the field of photovoltaics, such as building or vehicle integration require investigations of lightweight PV module concepts [1]. This research proposes and evaluates a lightweight PV module concept using glass fiber-reinforced polymers (GFRP) based on epoxy composites within the module stack. The usage of GFRP as front material as proposed in this work, reduces weight by 44–74 % compared to conventional glass-back sheet modules. We show results that with the proposed module stack hail impact resistant module can be built with small and large size avoiding any cell cracks after impact. Additionally, modules with GFRP front layer withstand thermal cycling tests with low power losses ranging from −0.9 % to −1.1 % at P_{mpp} depending on the individual GFRP layer. We also show results of cut susceptibility tests with an increased performance compared to modules with a polymeric front layer. Development topics remain as shown by damp-heat and UV irradiation testing, were an optimization of the module stack still needs to be performed.

1. Introduction

Previous studies introduced the theoretical potential of installed photovoltaics (PV) power for commercial vehicles [1–5]. Furthermore, it was also shown how the system performance ratio of such VIPV systems can be optimized [1]. Still, it remained a challenge to equipe commercial vehicles with impact-resistive, lightweight, highly transparent, and low-cost PV modules [1,5,6]. While other groups investigated the usage of glass fibers in encapsulant and back sheets [6,7], in this work we aim to investigate and provide a proof-of-concept for using glass fiber-reinforced polymers (GFRP) directly as a front-sheet for PV modules. The insufficient mechanical properties of polymer-based PV modules establish the need for new material investigations. Composite materials, such as reinforced polymers, have a high strength to weight ratio and are therefore often applied in high-performance, lightweight aerospace applications [8]. GFRP structures can provide excellent mechanical support to PV cells [6,7], while being less brittle and more elastic than glass panes [9]. Regarding module weight, a reduction of 30 % [10] up to 92 % [9] can be reached using GFRP front-sheets instead of conventional 3.2 mm glass. However, a major challenge is to realize high light transmittance, since applications with high transmittance composites are still underdeveloped [11–13].

2. Methodology

2.1. Fabrication of mini modules to evaluate GFRP module manufacturing concepts

Along the way towards an impact-resistive, lightweight, and highly transparent front-sheet, different approaches are investigated in this study. Three GFRP module manufacturing concepts are proposed and assessed as shown in Fig. 1. Whereas the first approach aimed to include glass fiber fabrics in front of the solar cells within two layers of encapsulant (a), the approaches (b) and (c) include glass fiber polymers as front-sheets and differ in the sourcing of these. While in (b) front-sheets are produced on laboratory scale in our facility by a vacuum infiltration, the front-sheets used in (c) are sourced from an industrial company. Further differences for approach (b) and (c) can be found in the next sessions. All three variants are supported from the rear side by a 1.5 mm GFRP backplate with an added gelcoat layer. Therefore, mini modules with a size of 20 cm × 20 cm featuring half-cut PERC solar cells are produced for the three approaches. More details are given in the following section.

Lamination is the most common and proven practice in PV module production. In this work, a one-level vacuum laminator E-LAPV from the company Meier Vakuumtechnik is used. For laminations in this work the encapsulant is chosen as Hanwha EVA HEP02. It is a crosslinking based,

* Corresponding author.
E-mail address: m.a.schueler@web.de (M.A. Schüler).

https://doi.org/10.1016/j.solmat.2024.113048
Received 30 April 2024; Received in revised form 24 June 2024; Accepted 18 July 2024
Available online 13 August 2024

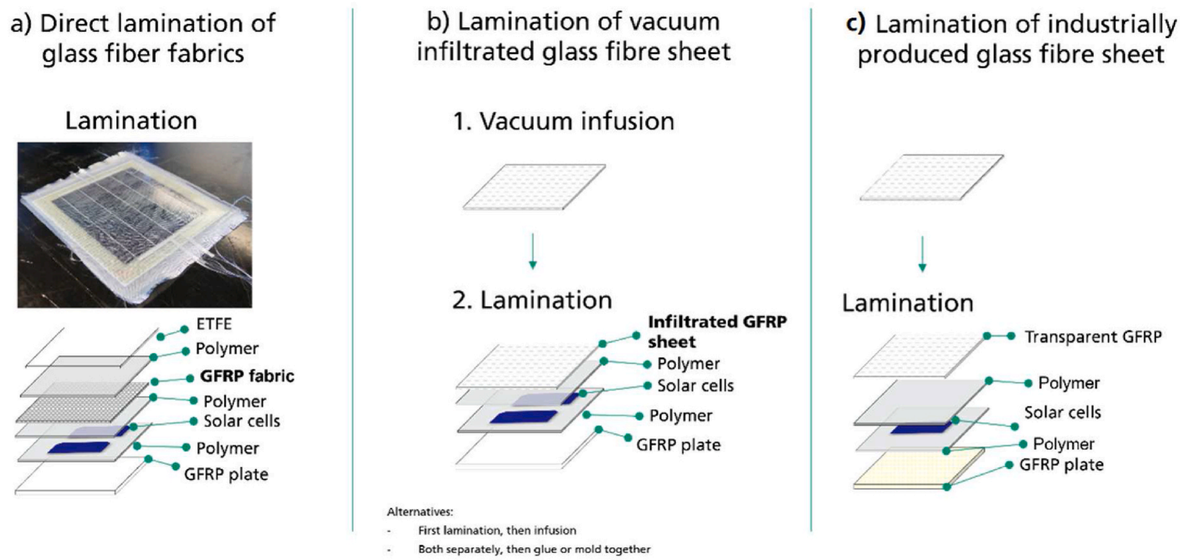

Fig. 1. Sketch of the three module concepts investigated in this research, showing direct fiber lamination (a), lamination of vacuum infiltrated glass fiber front-sheets (b) and lamination of industrially produced GFRP PV front-sheets (c).

Table 1
Module manufacturing matrix comprising six different configurations of two-, three- and six-layered GFRP front-sheets with different total areal GF weight, GFRP weight and GFRP thickness. Fiber values taken from Ref. [19].

Configuration	No. of samples	GF areal weight [g/m^2]	GFRP areal weight [g/m^2]	GFRP thickness [mm]
GFRP 1	6	560	763	0.58
GFRP 2a	6	840	1143	0.86
GFRP 2b	6	840	1143	0.86
GFRP 3	6	780	1062	0.82
GFRP 4	6	1170	1593	1.20
GFRP 5	6	624	849	0.60

solvent-free encapsulant with a thickness of 0.45 mm. The lamination temperature is adjusted to the EVA with 140 °C and a combined pressure of 800 mbar is applied for 30 min. The EVA crosslinks in a radical reaction into a three-dimensional polymer network and seals the modules accordingly [14].

2.2. Fabrication of the vacuum infiltrated glass fiber sheets

Configurations GFRP 1–5 as listed in Table 1, are produced on lab scale for the vacuum infiltrated front-sheets and have varied stacking sequence. Plain woven fabrics, comprising orthogonally woven fibers are stacked. GFRP 1 and GFRP 3 consist of two fiber layers, while GFRP 2a and GFRP 2b and GFRP 4 consist of three stacked fiber layers. Ideally, stacking sequences should be symmetric to the middle axis of the composite to prevent warping due to residual stresses [15–17]. GFRP 2a and GFRP 2b consist of the same number of fiber layers but while GFRP 2a

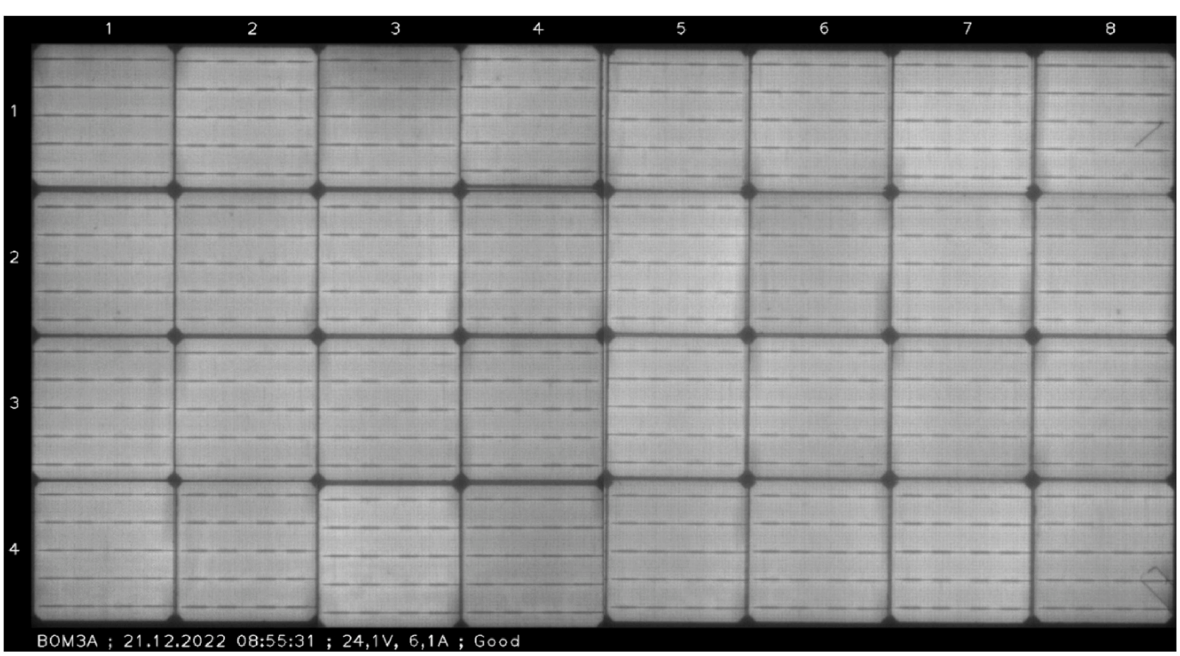

Fig. 2. Stitched EL Image of lightweight PV module with industrially produced GFRP front-sheet (dimensions: 670 mm × 1350 mm).

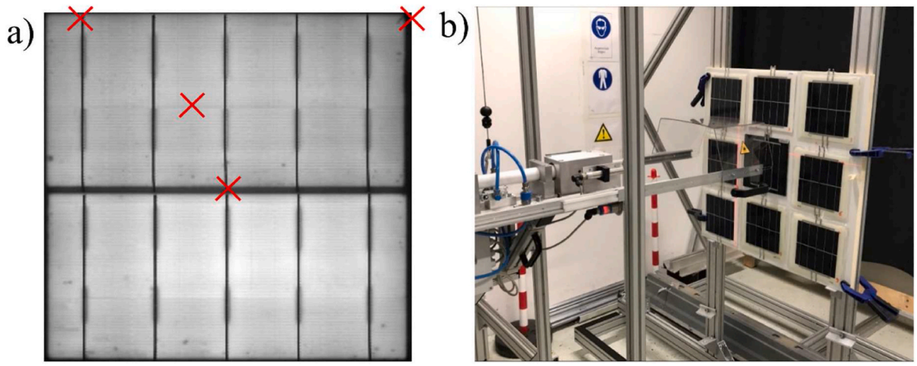

Fig. 3. Four hail impact locations selected for hail tests on two half-cell modules (left) and hail test setup (right) regarding IEC 61215 specification [22].

follows a quasi-isotropic stacking sequence, in GFRP 2b the fiber orientation is same in all 3 layers. Polymer matrices are used to stabilize the sensitive glass fibers, such can be Thermoplastics or Thermosets. While Thermoplastics seamed not suitable for the vacuum bagging process due to high viscosities and solid physical state at room temperature, Thermosetting polymers have lower viscosities and are liquid at room temperature, making them eligible for vacuum bagging infusion. Infusion epoxy resin IN2 with a cycloaliphatic amine-based hardener is chosen as the matrix material sourced from Easy Composites Ltd. Note, that the thickness of the sheets are measured and varied from 0.58 to 1.20 mm for the different configurations. The GFRP front-sheets manufactured in this research have areal weights in the range of 763–1593 g/m^2. Note, that typical solar front glasses with 3 mm thickness have weights around 7500 g/m^2 [18].

2.3. Lamination of the GFRP modules with industrially produced front-sheets

In addition to producing mini-modules sized 20 cm × 20 cm with half-cut PERC solar cells, larger modules where also produced to evaluate the stiffness and handling of GFRP front-sheets in an industrial PV module production. The modules with industrially produced sheets are laminated at our partner facility "Sunset Energietechnik GmbH" in two different sizes with an increased rear side support of a 1.9 mm GFRP backplate. The supplier of the industrial front-sheets tested different epoxy resin matrices and suggested to use two variations (GFRP "A" or "B") suitable for our intention. The first set of modules, intended for durability tests such as hail and thermal cycling, are produced in dimensions of 670 × 1350 mm, with four modules per GFRP variation. Two reference modules are produced with market available front-sheets based on PET, marked as PET “D” for the front-sheet DS392 by Dunmore with a thickness of 275 μm and PET “F” for the product Feron neoX PE 160 with a thickness of 160 μm. An electroluminescence (EL) image of a 32-cell module successfully built in this size is shown in Fig. 2. Modules produced for the cut susceptibility test are manufactured in dimensions of 220 mm × 720 mm, with four modules per GFRP variation as well.

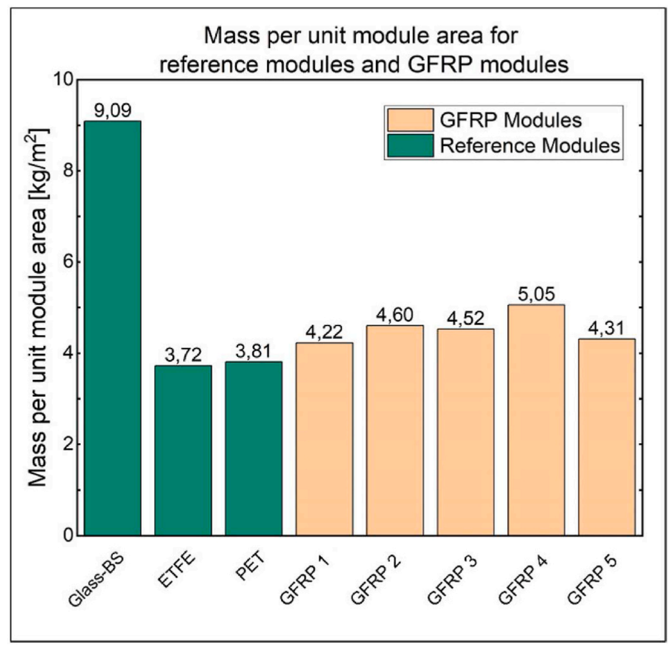

Fig. 5. Areal density in kg/m^2 for different reference modules (green) and GFRP module (orange) configurations.

2.4. Test procedures to evaluate the GFRP modules

After production, the samples were characterized under Standard Test Conditions (STC) to measure their power output and visually inspected for possible damages in an electroluminescence inspection at the short-circuit I_{SC}. The manufactured modules underwent separately several reliability tests such as the hail impact testing, 15 kWh/m^2 ultraviolet (UV) radiation, and 500 h of damp heat (DH) according to IEC 61215 [20], as well as accelerated thermal cycling (aTC) tests as described in Ref. [21].

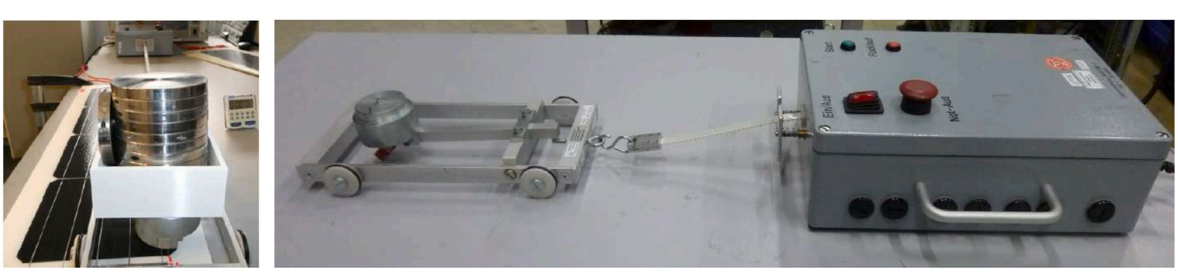

Fig. 4. Loaded metal blade which is dragged over the module frontside to simulate mechanical impact.

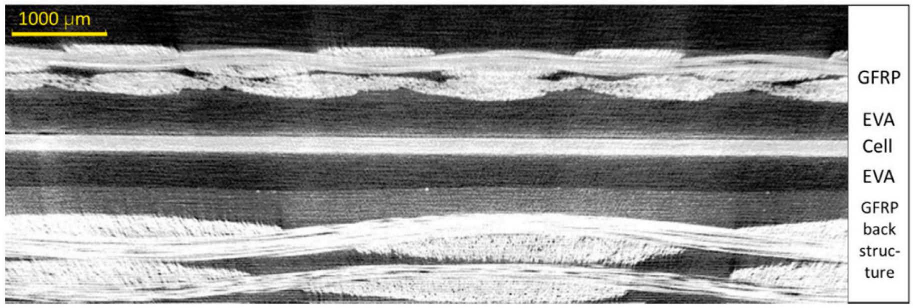

Fig. 6. Cross section of the semi-product GFRP produced with vacuum infusion of one layer of GF fabric with an areal density of 2 × 290 g/m^2.

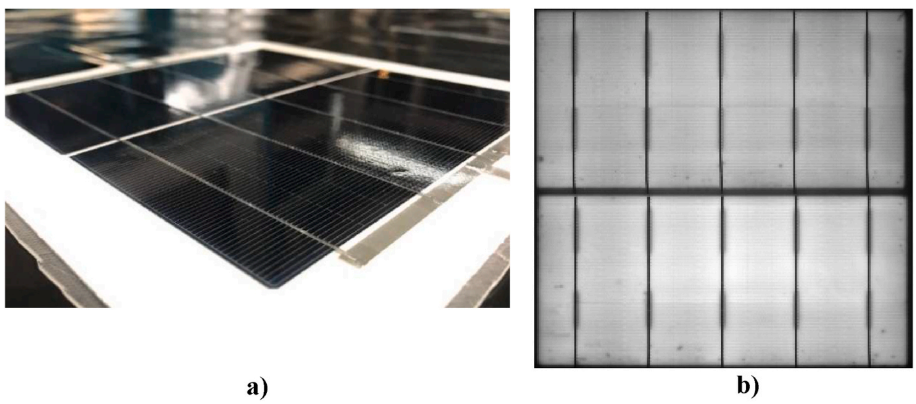

Fig. 7. Picture of produced mini modules with a pre-infused GFRP front-sheet in a) after lamination and b) the according electroluminescence measurement.

Hail impact tests are proceeded as regarding IEC 61215 with controlled speed of 23 m/s and a diameter of 25 mm and a weight of 7.53 g for the ice ball. Further all GFRP modules are fixed on a support structure which resembles the Trailerskin (GFRP-PU Sandwich) of the investigated application in LadePV) [3], as indicated in Fig. 3 b). As can be seen in Fig. 3 a) the mini modules with vacuum infiltrated front-sheets are exposed to four hail impacts.

Furthermore, the industrially produced modules undergo a mechanical load impact test on the front side, inspired by the IEC61730–2:2016 MST 12 "Cut Susceptibility". This test involves a metal blade that is subjected to gradually increased load using steel weights of 500 g, as shown in Fig. 4. After loading, the metal blade is dragged over the polymer surface at a speed of approximately 150 mm/s.

After each run, a visual inspection and a leakage current test are conducted in accordance with IEC 61215–2:2021. The test matrix for this test includes different front-sheet modules, such as polymer-based modules with ETFE of 250 µm thickness, two PET front-sheets with 275 µm and 300 µm, and two GFRP front-sheet modules with approximately 800 µm thickness.

3. Results and discussion

One of the main purposes of this research is to identify materials for lightweight modules while maintaining sufficient mechanical, thermomechanical, and optical properties. The average mass per unit module area for all composite and reference module configurations is determined by adding up the weights of all module components, assuming an inactive cell area of 5 % [23]. The results are plotted in Fig. 5. The mass

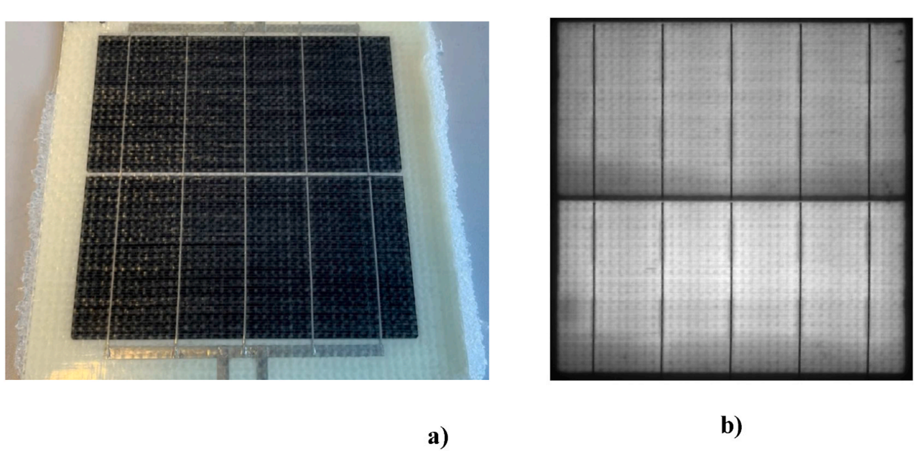

Fig. 8. Picture of produced mini modules with industrially manufactured GFRP front-sheets in a) after lamination and b) the according electroluminescence measurement.

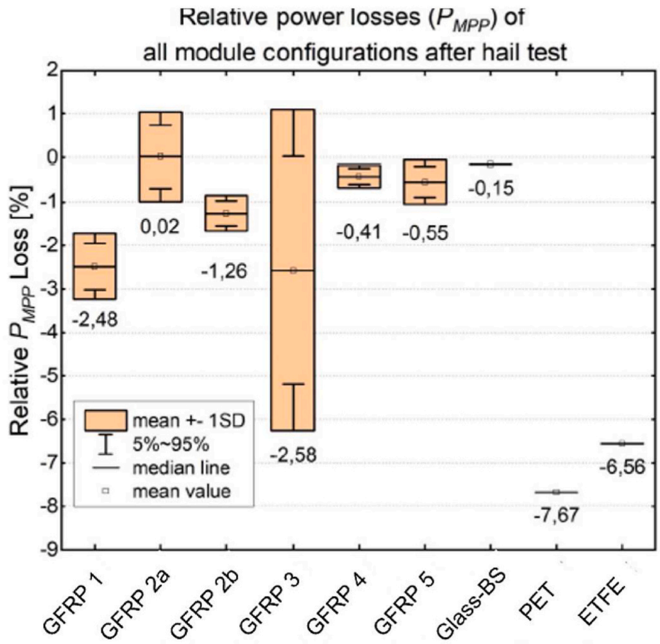

Fig. 9. Relative P_{mpp} losses after hail test for GFRP modules (orange) and reference modules (Glass-BS, PET, ETFE). The box plots incorporate data obtained from two samples for each GFRP variant and one module for the references.

per unit module area of typically 9.09–12.5 kg/m^2 for glass-BS references are found to be reduced by 44.4–53.5 %, depending on the applied GFRP configuration. Total module weights per unit area of 4.22–5.05 kg/m^2 are realized. When looking at the weight of the front-sheets only, the lab-scale GFRP achieves weight reductions of 78–90 % compared to a conventional 3.2 mm glass cover.

The IV-Characterization with STC revealed that PV modules manufactured with direct lamination or direct infusion of glass fiber fabrics and solar cells (concept seen in Fig. 1 a) exhibited insufficient optical coupling, air bubbles, dried passivation layers, and cracks in the solar cells, therefore high power losses of up to −65 %.

On the other hand, modules manufactured by laminating a pre-infused GFRP front-sheet on the PV module stack (concept seen in Fig. 1 b), results shown in Figs. 6 and 7) demonstrated remarkable optical coupling, maximum power losses of −4%, and low susceptibility to failures during the manufacturing process. Fig. 6 shows a cross section of the module with the GFRP layers clearly visible.

In addition, PV modules with conventionally produced transparent GFRP front-sheets (concept seen in Fig. 1 c), results shown in Fig. 8), with an adjusted glass-content of approximately 2 × 290 g/m^2 and two variants of highly transparent epoxy resin (GFRP A or GFRP B), were tested as state-of-the-art references. These modules showed average power losses of −8%. While the modules with GFRP semi-products and the ones with industrially produced GFRP front-sheets showed the most promising optical coupling, the modules produced through direct lamination were not considered further in this work due to insufficient optical coupling (see Fig. 9).

Table 3
El images and relative power changes ΔP_{mpp} after hail test of two samples each for the three different GFRP module configurations.

Layup	Sample 1	Sample 2
GFRP 1	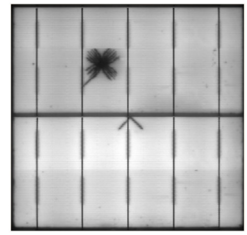	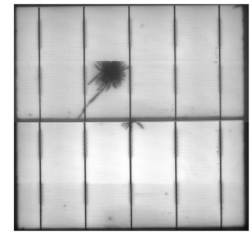
Δ P_{MPP}	−1.9 %	−3.0 %
GFRP 2a	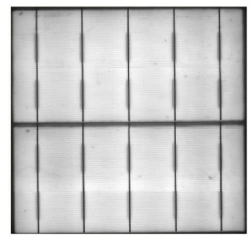	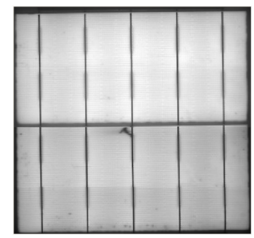
Δ P_{MPP}	+0.7 %	−0.7 %
GFRP 3	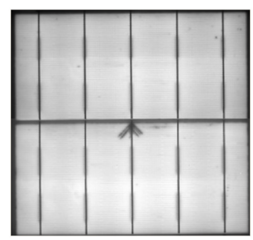	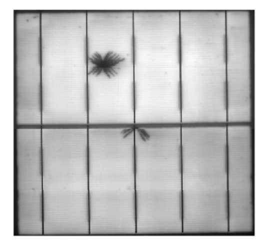
Δ P_{MPP}	−1.0 %	−1.6 %

3.1. Results of hail test procedures

Hail test according to IEC 61215 are proceeded for the vacuum infiltrated mini modules, as well as for the full-scale modules with conventional GFRP fronts. With four hail impacts on each minimodule produced, average hail-induced power changes of −1.2 % have been determined for all six invested vacuum-infiltrated GFRP module

Table 2
El images and relative power changes ΔP_{mpp} after hail test of one sample each for the three different reference module configurations.

Glass-BS	ETFE	PET
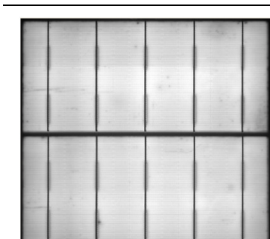	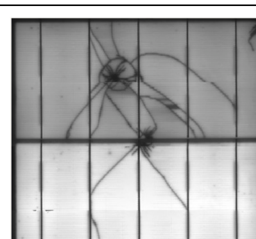	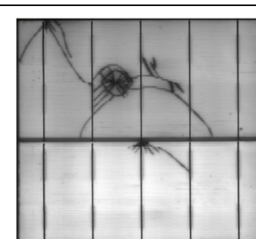
−0.2 %	−6.6 %	−7.7 %

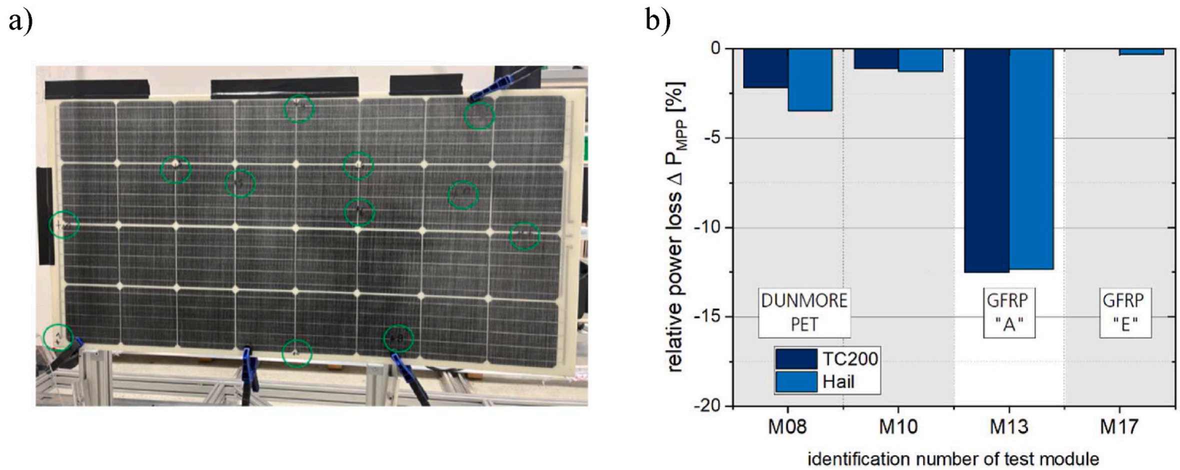

Fig. 10. Twelve hail impact locations selected for hail tests on full scale module regarding to specification IEC 61215 [7] indicated in green (a) and resulting power changes at P_{mpp} of the test matrix (b).

configurations. Finally, no impact-induced damages in the GFRP front-sheet have been identified with 3D X-ray microscopy. Initial sample modules are intact showing no cracks before hail testing. Thus, all cracks detected and shown in Table 2 for reference modules and Table 3 for GFRP modules are related to hail impacts. In addition, hail-induced relative P_{MPP} losses are given.

As presented in Table 2, the Glass-BS module does not show any cell damage after hail impact. The polymer modules show severe cell cracks at 3 out of 4 impact locations each. Cracks are significantly propagating through the cell area. The crack on the cell center is circumferential for both polymer-based modules. With visual inspection, dents in the diameter range of the hail impactor can be detected on the polymer front-sheets.

Severity of hail-induced damage patterns for the different module configurations is characterized by the relative P_{MPP} losses, as given Fig. 10 and indicated EL which are shown in Tables 2 and 3. The GFRP modules show generally a lower number of cracks or even no cracks, depending on the front-sheet configuration (see Table 3). Cell damage remains local, and no crack propagation is detected.

All Two-layered GFRP modules (GFRP 1 and 3) show higher average *PMPP* losses than three-layered GFRP modules (GFRP 2a, 2b and 4). It is noteworthy, that configuration GFRP 2a and 2b show less *PMPP* losses than configuration GFRP 3, even though the total GF weight and thickness are quite compatible in these configurations (see Table 1). This indicates a setup of an added fiber layer with less material density in the single layers, but improved number of crossed stacks can be beneficial for the robustness of the fiber front-sheet.

Both polymer-based reference modules show higher impact-induced P_{MPP} changes of −6.56 % (ETFE) and −7.67 % (PET), compared with all GFRP module configurations. GFRP modules show an average relative P_{MPP} change of −1.21 %, while a maximum average relative P_{MPP} change of −3.02 % is observed for sample 2 in configuration 1.

Please note, the accuracy and reproducibility of the relative power change measurements at *PMPP* are in the range of ±1 %.

The industrially produced GFRP modules are also subjected to testing, starting with 200 thermal cycles before exposure to hail, according to IEC61215-2. Twelve specific points or areas of interest are defined on the lightweight modules, as indicated in Fig. 10 a). The resulting P_{mpp} measurements, relative to the initial power characterization, are shown in the graph provided in Fig. 10 b). It is noteworthy that the reference module produced with a market-available front-sheet DS392 by Dunmore (further annotated ass PET "D") successfully passed the full sequence, as its relative power changes were below −5%. Fig. 11 shows EL images of the 3 shown modules, where it is visible that the reference module PET "D" suffers damage to the solar cells from the hail impact, while still passing the sequence regarding the power loss requirement below 5 %. However both GFRP modules do not suffer any damage to the solar cell resulting from the hail impact. Apparently, GFRP suffered a degradation from TC, resulting in this significant power loss.

3.2. Results of cut susceptibility tests featuring industrially produced GFRP front-sheets

Prior to the metal blade test, all modules are inspected for cell cracks using an electroluminescence test, which is also conducted after each iteration. The Cut Susceptibility Test begins with a force of 8.9 N (~0.9 kg) applied to the metal blade, and then the weight exposed to the blade is increased by 0.5 kg in each iteration. After each iteration, the modules are visually checked and undergo a wet leakage test. A summary of the four iteration steps is presented in Table 4. Initially, all modules showed no cracks. However, as the weight exposed to the blade increased to 2.9 kg and 3.4 kg, the polymer-based modules exhibited severe damage at the cell level, but still passed the isolation test. The ETFE-based modules failed the isolation test after exposure to 4.4 kg. On the other hand, the PET modules from two different suppliers (Dunmore as PET "D" and Feron as PET "F") passed until 9.4 kg and 6.4 kg, respectively. Overall, the BOM GFRP "B" performed the best as it passed the test limit of 10.4 kg. The second BOM GFRP "A" passed until 8.4 kg but failed to pass the isolation test afterwards. However, no failures were observed in the electroluminescence test.

3.3. Results of reliability test procedures

After 200 accelerated thermal cycles (aTC), GFRP modules with vacuum-infiltrated sheets exhibited minimal warping and low power changes ranging from −0.9 % to −1.1 % at P_{mpp}. In contrast, reference modules with glass-backsheet (BS) setup, PET front-sheets, or ETFE front-sheets experienced higher power changes of −3.2 %, −3.5 %, and −34 %, respectively. The improved thermomechanical resistance of vacuum-infiltrated GFRP modules can be attributed to a lower coefficient of thermal expansion (CTE) mismatch with other module components and the additional stiffness provided by the GFRP front-sheets.

Two samples each of the configurations GFRP 1, GFRP 2 and GFRP 3 are subjected to UV irradiation of 15 kWh/m^2. Visible inspection reveals strong yellowing of all modules, as depicted in Fig. 12 for configuration GFRP 3, exemplary. Yellowing after UV test is significantly more intense than yellowing observed after aTC200.

After UV exposure, samples are IV characterized and relative changes are detected in the range of −11.7 to −12.6 % is detected at P_{MPP}. The

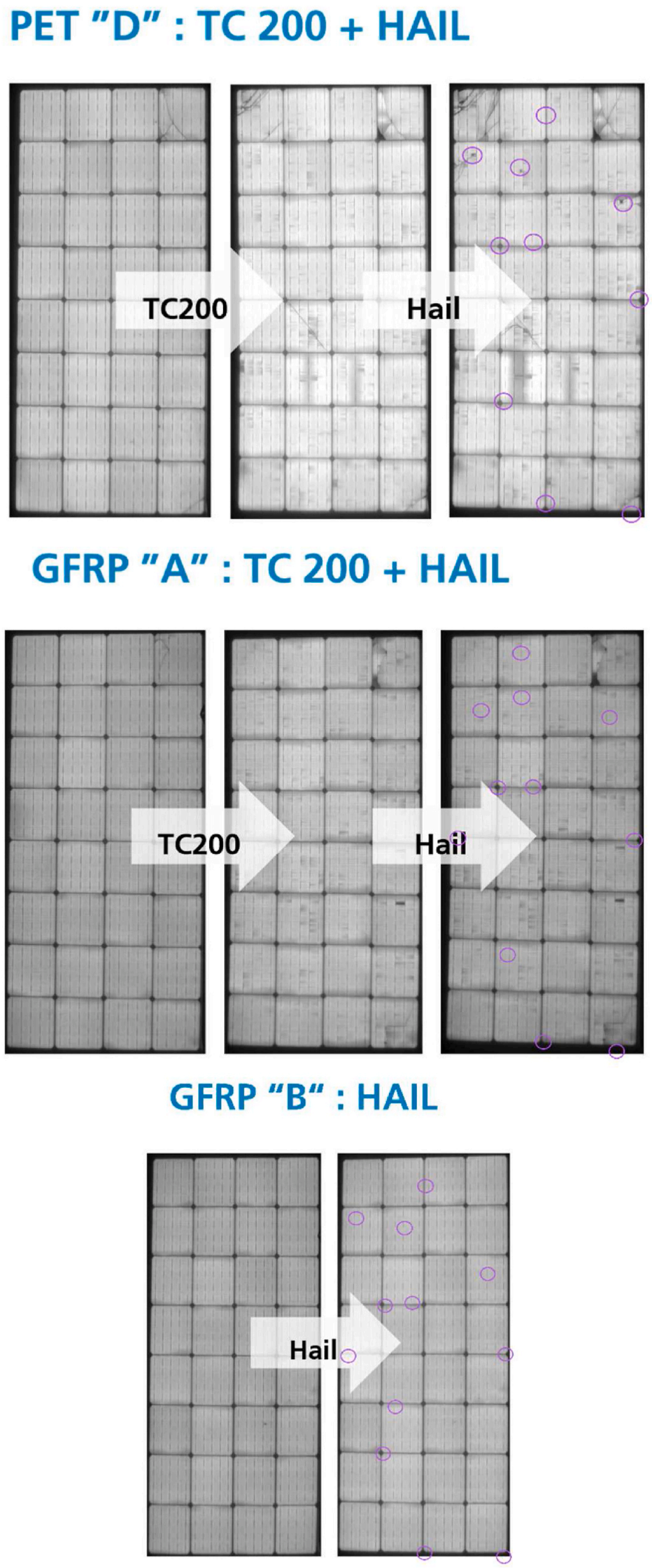

Fig. 11. Photographs of EL measurements initially and after individual sequence steps. Results are given for PET "D" and GFRP "A" after 200 thermal cycles and hail test and resulting EL before and after hail impact (purple dots) for GFRP "B".

Table 4
Relevant properties to determine flexural modulus E_f of a sample module. Taken from [61].

Property	Symbol	Unit
Load change	ΔF	N
Deformation (crosshead travel)	Δs	mm
Sample width	b	mm
Support bar span	L	mm
Sample thickness	h	mm

major cause of the power losses are decreased transmittance due to be increased reflection or absorption within the front-sheets, resulting in decrease of I_{SC} and I_{MPP}. Meanwhile, V_{OC}, V_{MPP} and FF remain mostly constant. Exemplary, the IV-curves of configuration GFRP 3 before and after UV testing is shown in Fig. 13.

As for a limited number of mini modules produced, the samples exposed to DH500 have been previously hail tested. Thus, some of the modules have initial cell cracks. During DH500, all modules with existing cracks reveal crack propagation, such as for the reference modules with PET or ETFE. Measurements reveal P_{MPP} changes are in the range of −0.9 % to −2.7 % for reference modules, and in the range of −3.9 % to −8.0 % for GFRP mini modules. Isolated influence of humidity propagating into the modules could be a potential issue as well as insufficiently high water-vapor transmission rates of the GFRP layer.

In parallel, industrially produced GFRP front-sheets demonstrated significant power changes of up to −20 % at P_{mpp} after 200 aTC cycles. The higher power losses using these sheets can be attributed to inhomogeneous thermal expansion caused by random spread fiber layers, which is particularly critical at the resin to fiber interfaces. Furthermore, testing the industrially produced GFRP front-sheets with an added gelcoat protection layer for 15 kWh/m^2 UV radiation also resulted in significant power changes of up to −7.5 % at P_{mpp}.

4. Conclusion

This research serves as a proof-of-concept study for the design of lightweight and impact-resistant PV modules using GFRP front-sheets with promising optical transmission. Provided that the GFRP front-sheets can cost-efficiently be produced on a large scale, the GFRP module manufacturing concept remains very close to the standard lamination process of PV modules by simply replacing the polymer-based front-sheet foil with a GFRP semi-product. The study suggests different concepts for GFRP front-sheets achieving sufficient mechanical and optical properties, while enabling weight reductions of 44–74 % compared to Glass-BS modules. One significant finding from the mechanical impact tests on the GFRP modules is that they exhibited improved impact resistance, with a low occurrence of local, less severe, and non-propagating cell cracks compared to polymer-based front-sheet modules. Various fiber-layers with varying stacking sequences and glass-fiber have been tested on mini-modules (GFRP1 to GFRP 5). Local cracks can be detected in the mini modules, as it is the case for the polymer-based front-sheet modules.

Compared to the polymer-based references, GFRP modules show lower number of cracks, no crack propagation and star shape of the cracks indicate a global impact energy dissipation in many directions in the composite front-sheet. In the polymer-based modules, cracks do not remain local, but significantly propagate through the cell area leading to change in P_{MPP} of −6.56 % for the ETFE and −7.67 % for the PET front-sheet module. For all the mini modules tested, the impact location between the two half cells and the cell center appears to be the most vulnerable ones. In our investigation, every GFRP configuration in the mini modules that reveals cell cracking showed them in the earlier mentioned spots. The impact point on the cell edge seems to be less prone. While local peak impacts occasionally reach the cell causing small cell cracks, the higher rigidity of GFRP compared to ETFE and PET

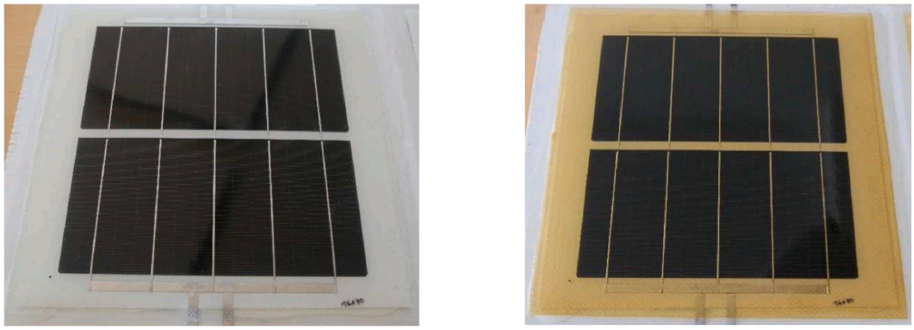

Fig. 12. Photographs of module configuration GFRP 3 (left) before and (right) after applying 15 kWh/m^2 UV irradiation showing strong yellowing. Consequently, P_{MPP} changes of −11.8 % are measured.

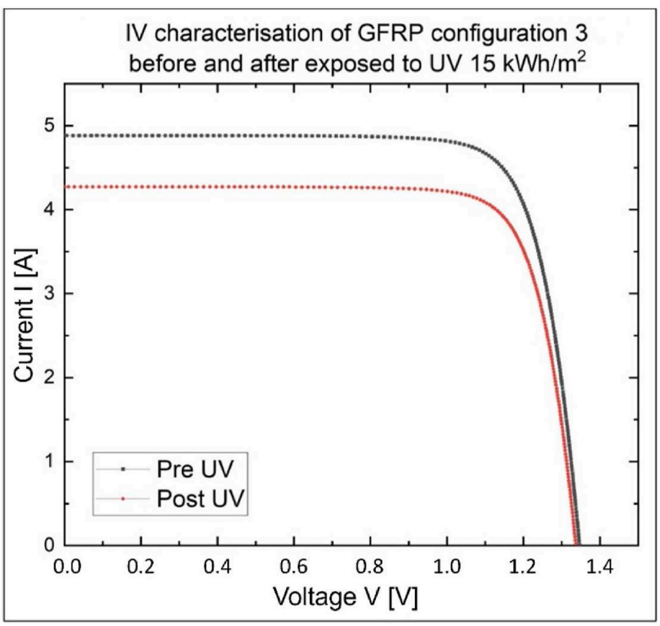

Fig. 13. Resulting IV curves for exemplary module configuration GFRP 3 before and after exposure to UV15 kWh.

may enhance impact resistance and local energy dissipation. The three-layered setup GFRP 2a seemed to perform best in Hail tests.

Based on this investigation, the information on glass content and stacking is transferred to an industrial GFRP sheet producer (GFRP A and GFRP B) leading to good results after hail impact tests where no cell cracks could be detected. Note, that the hail test results for the industrial modules could be partly influenced by the increased rear-side support from 1.5 mm to 1.9 mm GFRP backplates.

For thermal cycling tests we found that the vacuum-infiltrated front-sheets were able to overcome differences in thermal expansion, resulting in power changes below −1.1 % during thermal cycling but at least one of the industrial GFRP front-sheets showed an issue and resulted in a power loss higher than 12 %.

It is noteworthy, that the modules with GFRP front-sheet showed a significant improvement when tested against polymeric front-sheets (PET and ETFE) in cut susceptibility tests.

Further development is necessary for the optimization of the module stack against humidity and UV exposure. Our investigations indicate Gelcoat (or other protective layers) can have a positive effect for UV stability, as seen from comparing power changes after exposure, between minimodules with infiltrated GFRP (−11.7 % to −12.6 %) and industrially produced with the later one's seam to suffer less (−7.5 %). However, the losses are still too high, and a further optimization is necessary. IV Characterization after exposure to 500h of DH to the mini modules showed power changes of −3.9 % to −8.0 % and further development and investigation is needed to obtain humidity resistive modules.

Future research in this area will focus on addressing the challenges of improving UV and damp heat resistance in GFRP front-sheets, while still maintaining a strong mechanical impact as well as thermal changes resistance of the setup. Variations in the resin and encapsulation as well as in the overall module stack will be explored to enhance optical transmission and resilience to environmental impacts in conventional fiber-based sheets, with the aim of developing lightweight PV front-sheets for commercial applications.

Data availability

The data that support the findings of this study are available from the corresponding author upon reasonable request.

CRediT authorship contribution statement

Marc Andre Schüler: Writing – original draft, Project administration, Methodology, Investigation, Conceptualization. **Mark-David Goth:** Resources, Investigation, Data curation. **Jochen Markert:** Visualization, Investigation, Data curation. **Luis Eduardo Alanis:** Visualization. **Christoph Kutter:** Project administration, Conceptualization. **Felix Basler:** Conceptualization. **Martin Heinrich:** Writing – review & editing, Writing – original draft, Funding acquisition. **Dirk Holger Neuhaus:** Writing – review & editing, Funding acquisition.

Declaration of competing interest

The authors declare the following financial interests/personal relationships which may be considered as potential competing interests: Marc Andre, Schueler reports financial support was provided by Fraunhofer Institute for Solar Energy Systems ISE. Mark-David, Goth has patent #F63139 pending to German. If there are other authors, they declare that they have no known competing financial interests or personal relationships that could have appeared to influence the work reported in this paper.

Acknowledgements

The authors would like to thank former colleague Christoph Kutter and the team-leader Li Carlos Rendler, as well as Jörn Müller from Lamilux for fruitful discussions. Aswin Linsenmeyer from Sunset Energietechnik is gratefully acknowledged for manufacturing of the test modules with Industrial produced GFRP front-sheets. This work was funded by the German Ministry of Economic Affairs and Energy under Grant No. 03EE1002A "Lade-PV".

References

[1] M. A. Schüler, C. Kutter, L. E. Alanis, L. Saroch, C. Barz, J. Bornwasser, S. Reichert, H. Neuhaus, M. Heinrich, High-voltage vehicle integrated photovoltaic system concept and demonstrator truck: presented at WCPEC-8, 8th world conference on photovoltaic Energy Convers., 26-30 September 2022, Milan, Italy.

[2] M. Heinrich, A.J. Beinert, P. Romer, L.C. Rendler, F. Basler, S. Wendlandt, D. H. Neuhaus, Approaches for a lightweight module with laminated materials, in: Proceedings of the 38th European Photovoltaic Solar Energy Conference and Exhibition, EU PVSEC), Lissbon, 2021, pp. 761–764.

[3] C. Kutter, F. Basler, D.H. Neuhaus, M. Heinrich, J. Markert, L.E. Alanis, Integrated lightweight, glass-free PV module technology for box bodies of commercial trucks, in: 37th EUPVSEC European PV Solar Energy Conference and Exhibition, Lisbon, Portugal, 2020, pp. 1711–1718, in: https://www.eupvsec-proceedings.com/proceedings?fulltext=kutter&paper=49165.

[4] Jonathan Govaerts, Tom Borgers, Arvid van der Heide, "On the road towards vehicle integration: glass-fibre reinforced encapsulation enabling light-weight and curved PV modules," 37th EUPVSEC European PV Solar Energy Conference and Exhibition, 7-11 September 2020, Lisbon, Portugal.

[5] Bin Luo, Jonathan Govaerts, Rik Van Dyck, Tom Borgers, Bart Ruttens, Marta Casasola Paesa, Jan D'Haen, Loic Tous, Hariharsudan Sivaramakrishnan Radhakrishnan, Michael Daenen, Aart Willem Van Vuure, Jef Poortmans, Development and thermo-mechanical reliability assessment of fiber reinforced polymers in lightweight PV modules towards vehicle-integrated photovoltaics, Sol. Energy Mater. Sol. Cell. 259 (2023) 112455. https://www.sciencedirect.com/science/article/pii/S0927024823002763.

[6] J. Govaerts, B. Luo, T. Borgers, R. van Dyck, A. van der Heide, L. Tous, A. Morlier, F. Lisco, L. Cerasti, M. Galiazzo, J. Poortmans, Development and testing of light-weight PV modules based on glass-fibre reinforcement, EPJ Photovolt. 13 (2022) 13.

[7] B. Luo, J. Govaerts, R. van Dyck, T. Borgers, B. Ruttens, M.C. Paesa, J. D'Haen, L. Tous, H.S. Radhakrishnan, M. Daenen, A.W. van Vuure, J. Poortmans, Development and thermo-mechanical reliability assessment of fiber reinforced polymers in lightweight PV modules towards vehicle-integrated photovoltaics, Sol. Energy Mater. Sol. Cell. 259 (2023) 112455. https://www.sciencedirect.com/science/article/pii/S0927024823002763.

[8] K. Ravi-Chandar, Design Optimization and Characterization of Helicoidal Composites with Enhanced Impact Resistance, 2011.

[9] A. Reinders, H. de Wit, A. de Boer, Design of fibre reinforced PV concepts for building integrated applications, Department of Design, Production and Management (2009). https://www.researchgate.net/publication/236846392_Design_of_fibre_reinforced_PV_concepts_for_building_integrated_applications.

[10] C. Pascual, J. de Castro, A. Schueler, T. Keller, Integration of dye solar cells in load-bearing translucent glass fiber-reinforced polymer laminates, J. Compos. Mater. 51 (7) (2017) 939–953.

[11] A.S. Budiman, R. Sahay, K. Agarwal, R. Fajarna, F.E. Gunawan, A. Baji, N. Raghavan, "Modeling impact mechanics of 3D helicoidally architected polymer composites enabled by additive manufacturing for lightweight silicon photovoltaics technology," (eng), Polymers 14 (6) (2022).

[12] A. Reinders, H. de Wit, A. de Boer, "Design of fibre reinforced PV concepts for building integrated applications," Department of Design, Prod. Manag. (2009).

[13] T. Gorter, A.H.M.E. Reinders, A comparison of 15 polymers for application in photovoltaic modules in PV-powered boats, Appl. Energy 92 (2012) 286–297. https://www.sciencedirect.com/science/article/pii/S0306261911007033.

[14] S. Yakovlev, I. Dmitriev, E. Schebet, K. Emtsev, D. Andronikov, D. Orekhov, I. Shakhray, Lightweight Glass-free Solar Modules Based on Polycarbonate and Fiberglass Protective Sheets, 2021 (eng).

[15] A.S. AlOmari, K.S. Al-Athel, A.F.M. Arif, F.A. Al-Sulaiman, Experimental and computational analysis of low-velocity impact on carbon-, glass- and mixed-fiber composite plates, J. Compos. Sci. 4 (4) (2020) 148.

[16] J. Rivera, N.A. Yaraghi, W. Huang, D. Gray, D. Kisailus, Modulation of impact energy dissipation in biomimetic helicoidal composites, J. Mater. Res. Technol. 9 (6) (2020) 14619–14629. https://www.sciencedirect.com/science/article/pii/S2238785420319104.

[17] C. Kasapoglou, Design and Analysis of Composite Structures: with Applications to Aerospace Strucutres, Wiley, Chichester, West Sussex, U.K, Hoboken, NJ, 2010.

[18] AGC Glass Europe, Sunmax Premium Range: Arsenic- and antimony-free ultra low-iron float glass for solar applications. [Online] Available: https://www.agc-solar.com/applications/photovoltaics/. Accessed on: Jun. 17 2024.

[19] HP-Textiles GmbH, Lieferprogramm, 2017.

[20] IEC 61215-1, IEC 61215-1:2021 Terrestrial Photovoltaic (PV) Modules – Design Qualification and Type Approval – Part 1: Test Requirements, 2021.

[21] C.H. Schiller, L.C. Rendler, D. Eberlein, G. Mülhöfer, A. Kraft, D.H. Neuhaus, Accelerated TC test in comparison with standard TC test for PV modules with ribbon, wire and shingle interconnection, in: Proceedings of the 36th European Photovoltaic Solar Energy Conference and Exhibition, EU PVSEC, Marseille, France, 2019, pp. 995–999.

[22] IECON 2013 - 39th Annual Conference of the IEEE Industrial Electronics Society, IEEE, Nov. 2013 - Nov. 2013.

[23] L. Rakocevic, R. Gehlhaar, T. Merckx, W. Qiu, U.W. Paetzold, H. Fledderus, J. Poortmans, Interconnection optimization for highly efficient perovskite modules, IEEE J. Photovoltaics 7 (1) (2017) 404–408.